

IN-SITU MONITORING OF THE FORCE-OUTPUT OF FLUID DAMPERS: EXPERIMENTAL INVESTIGATION

Dimitrios Konstantinidis¹, Nicos Makris² and James M. Kelly³

ABSTRACT

This paper presents results from a comprehensive experimental program on fluid dampers in an effort to extract their force output during cyclic loading by simply measuring the strain on the damper housing and the end-spacer of the damper. The paper first discusses the path of stresses within the damper and subsequently via the use of elasticity theory shows that the experimental data obtained with commercially available strain gauges yield a force output of the damper that is in good agreement with the force output from the load cell. The experimental data show that the proposed arrangement is promising for monitoring in-situ the force output of fluid dampers and detect possible loss of their energy dissipation function.

INTRODUCTION

The rapid success of fluid dampers as seismic protection devices, in association with the increasing need for safe bridges has accelerated the implementation of large-capacity damping devices in bridges. For instance, the Vincent Thomas suspension bridge, the Coronado bridge and the 91/5 highway overcrossing (Delis et al. 1996, Makris and Zhang 2004) all three in southern California, the Bay Bridge and the Richmond-San Rafael bridge in northern California, as well as the Rion-Antirion cable-stayed bridge (Papanikolas 2002) in western Greece are all examples of bridges that have been equipped with fluid dampers.

The main challenge with fluid dampers is whether they will maintain their long-term integrity when placed in such large structures which are subjected to a variety of loads, appreciable dynamic displacements and long-term deformation patterns. Whereas large displacements and velocities are expected during earthquake loading, a prolonged wind loading would increase substantially the temperature of the damper. Similarly, traffic loading which induces vibrations of small amplitude but very long duration may fatigue the damper and eventually be detrimental in the event that installation imperfections are present as was experienced with the fluid dampers installed in the Vincent Thomas Bridge in southern California.

In this paper, we present an experimental investigation which examines the feasibility to measure the force-output of fluid dampers by only reading strains from strain gauges that are connected on the damper casing and the steel spacer placed between the double-ended damper and its attachment.

¹ Dept. of Civil and Environmental Engineering, University of California, Berkeley, CA

² Dept. of Civil Engineering, University of Patras, Greece

³ Dept. of Civil and Environmental Engineering, University of California, Berkeley, CA

PATH OF STRESSES DURING CYCLIC LOADING OF A FLUID DAMPER

Figure 1 shows a photograph of a medium size fluid damper (Force output = 250 kips at piston velocity = 42 in/sec) that is mounted on the U. C. Berkeley damper testing machine located at the Richmond Field Station. One end of the damper is connected to the actuator that is imposing the Motion, while the other end of the damper is stationary (see Figure 1). The damper shown in Figure 1 is identical to the eight dampers installed for the seismic protection of the 91/5 overcrossing located in Orange County, California (Makris and Zhang 2004). It is a double-ended damper in which the piston rod extends in both chambers of the damper on shown schematically in Figure 2 in order to achieve a symmetric mechanical behavior.

Figure 2 also shows schematically the stressing of the damper casing during tension and compression of the piston rod. When the piston rod is in tension (case 1) the damper casing is subjected to longitudinal tension; while, when the piston rod is in compression the compressive force is transferred directly at the end of the damper (spacer) via the pressurized fluid at the back chamber; therefore, only tangential (hoop) stresses develop during the bursting of the damper.

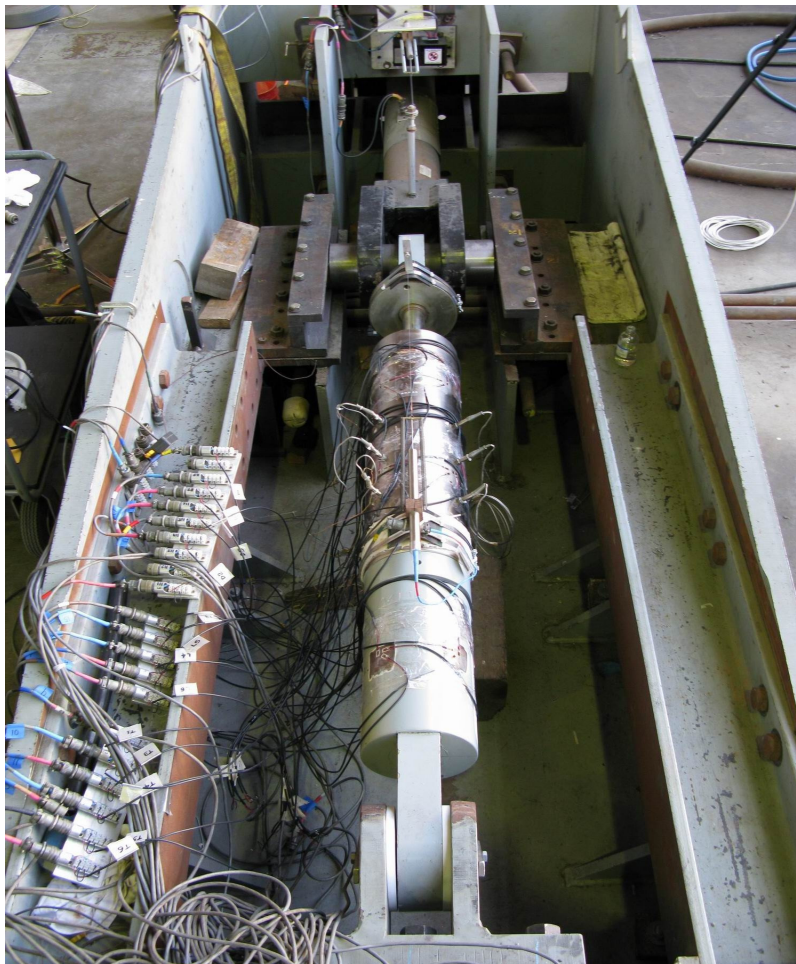
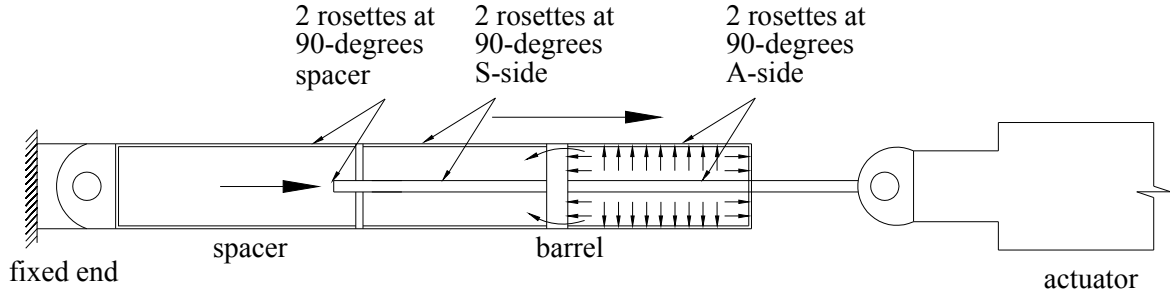


Fig. 1. View of the fluid damper mounted on the damper testing machine at the Richmond Field Station.

1) Piston Rod in Tension



2) Piston Rod in Compression

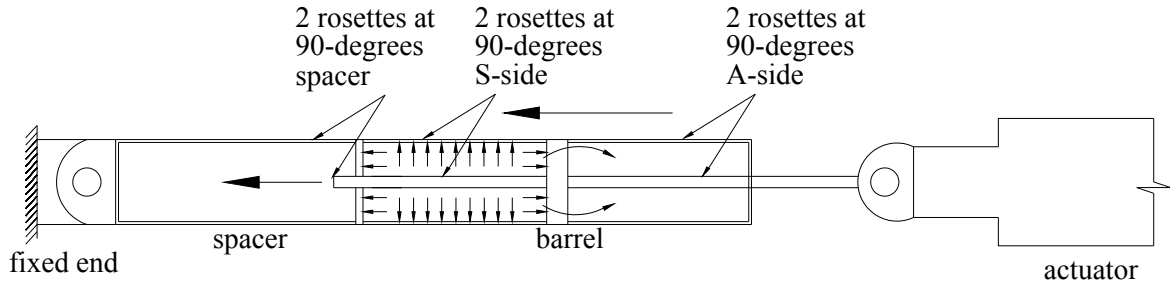


Fig. 2. Schematic of the cross-section of a fluid damper showing the stressing of the damper casing during tension of the piston rod (top) and compression (bottom).

INSTRUMENTATION OF THE DAMPER AND FORCE CALCULATION

The damper casing and the end-spaces are instrumented with strain gauges at the locations shown in Figure 2. Figure 3 shows a close-up view of a strain rosette where one strain gauge is installed along the longitudinal direction of the cylinder, one along the tangential direction of the cylinder and one installed at an angle. In the event that the damper is stressed purely axially without inducing any end moments and shear forces the longitudinal and tangential strain gauge measure principal strains. The strain rosette arrangement shown in Figure 3 has been used to check whether the longitudinal and transverse strains are indeed principal (Timoshenko 1970).

The spherical attachments of the test damper shown in Figure 1 eliminate the developments of any end moment or shear force; therefore, the principal directions of deformation are the longitudinal direction $= \epsilon_{xx}$ and the tangential direction $= \epsilon_{\theta\theta}$ of the cylindrical casing. The principal stresses σ_{xx} and $\sigma_{\theta\theta}$ may be then calculated from Hooke's law

$$\sigma_{xx} = \frac{E(\epsilon_{xx} + \nu\epsilon_{\theta\theta})}{1 - \nu^2} \quad (1)$$

$$\sigma_{\theta\theta} = \frac{E(\varepsilon_{\theta\theta} + \nu\varepsilon_{xx})}{1 - \nu^2} \quad (2)$$

where E and ν are the Young's modulus and Poisson's ratio of the steel of the damper casing. The force output of the damper is deduced directly as

$$P = \frac{\pi}{4} \sigma_{xx} (d_o^2 - d_i^2) \quad (3)$$

where d_o and d_i are the inner and the outer diameters of the damping casing. Table 1 offers selected geometrical characteristics of the damper casing.

In terms of the experimentally measured strains the force output is given by

$$P = \frac{\pi}{4} \frac{E(\varepsilon_{xx} + \nu\varepsilon_{\theta\theta})}{1 - \nu^2} (d_o^2 - d_i^2) \quad (4)$$

Table 1. Geometrical characteristics of dampers and selected physical properties of the steel casing.

Quantity	250-kip damper
Damping coefficient, C	1089.9 kN(sec/m) ^{0.35} (67.5 kip (sec/in.) ^{0.35})
Thickness of damper housing, ε	2.97 x 10 ⁻² m (1.17 in.)
Piston diameter, d_p	1.49 x 10 ⁻¹ m (5.87 in.)
Rod diameter, d_r	5.66 x 10 ⁻² m (2.230 in.)
Area of piston head, A_p	1.50 x 10 ⁻² m ² (23.19 in. ²)
Cross-sectional area of spacer, A_s	2.30 x 10 ⁻² m ² (35.7 in. ²)
Maximum stroke, U_o	0.203 m (8 in.)
Young's modulus, E	30000 ksi (207 GPa)
Poisson's ratio, ν	0.3

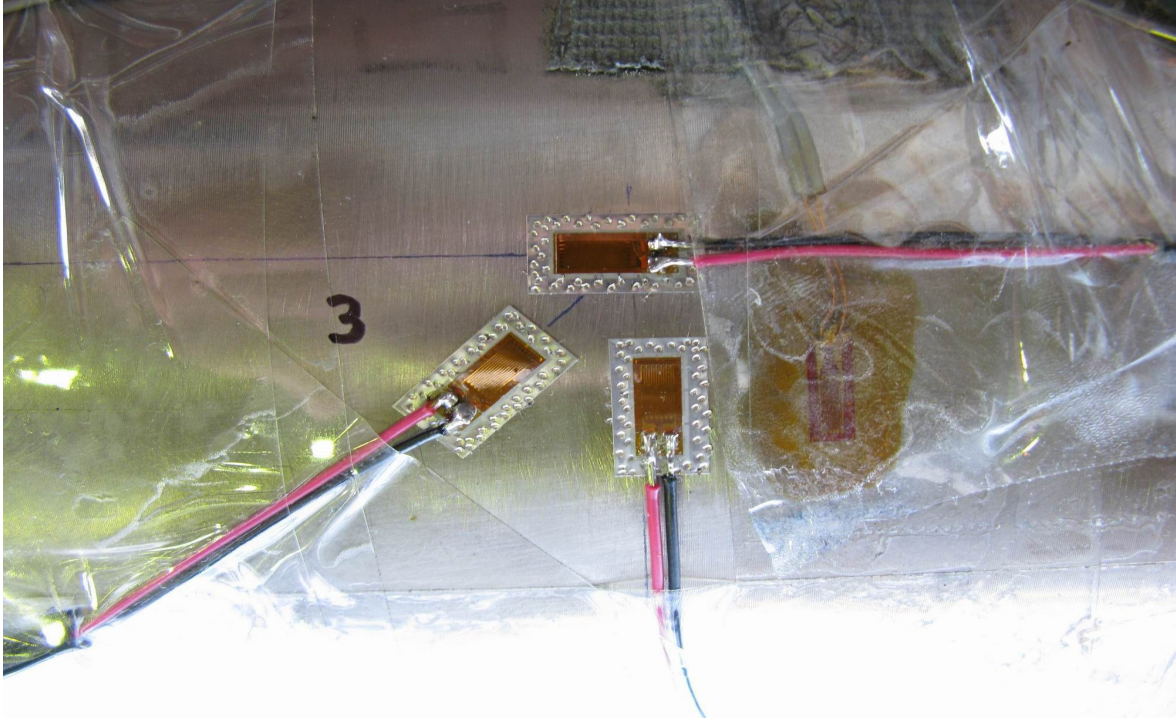


Fig. 3. Close-up view of a strain rosette mounted on the casing of a fluid damper

EXPERIMENTAL PROGRAM AND INTERPRETATION OF DATA

The experimental set-up shown in Table 1 was used to investigate the potential of the proposed methodology. Figure 4 show recorded force-displacement loops when the damper is subjected to a harmonic displacement history, $u(t) = u_o \sin(2\pi ft)$ with $u_o = 0.5$ in. and $f = 0.5$ Hz. The darker loops are associated with the force recorded from the load cell while the lighter half loops are those extracted from the strain gauges attached on the damper casing.

Figure 5 show recorded force-displacement loops when the damper is subjected to the same harmonic displacement history ($u_o = 0.5$ in. and $f = 0.5$ Hz). Now the loops extracted from the strain gauges attached on the spacer offer the force levels very close to those obtained with the load cell. The fidelity of this procedure is acceptable even for motions with low amplitude. For instance Figure 6 show recorded force-displacement loops when the damper is subjected to a harmonic force with $u_o = 0.2$ in. and $f = 1.0$ Hz.

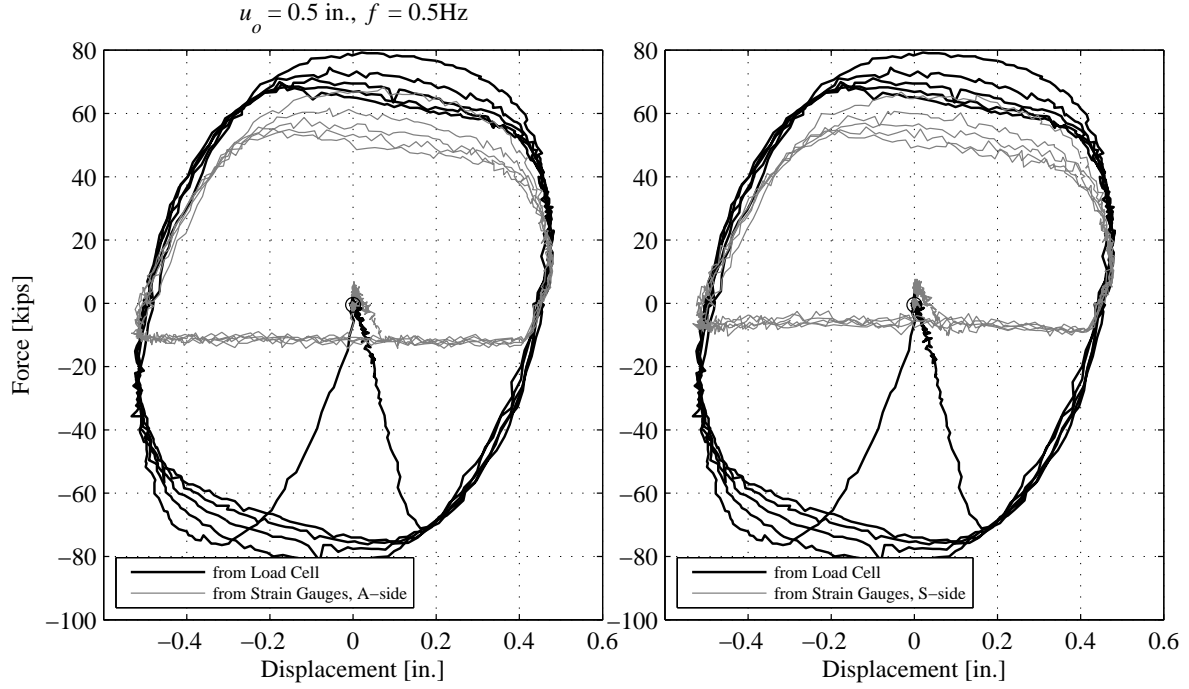


Fig. 4. Hysteresis loops with the force as measured with the load cell (heavy line) and as calculated from measured strains (light line) from strain gauges welded on the A-side (left graph) and the S-side (right graph) of the damper.

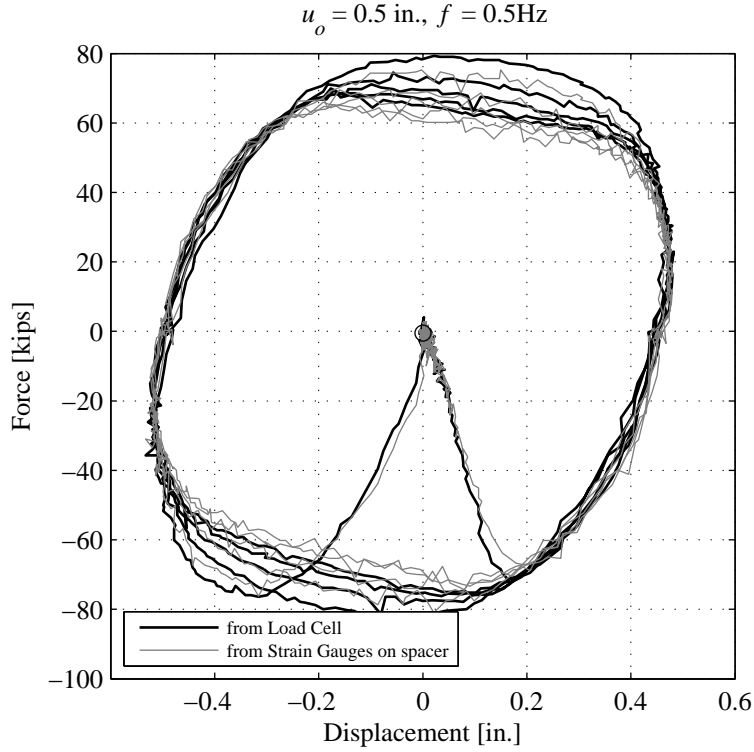


Fig. 5. Hysteresis loops with the force as measured with the load cell (heavy line) and as calculated from measured strains (light line) from strain gauges welded on the spacer.

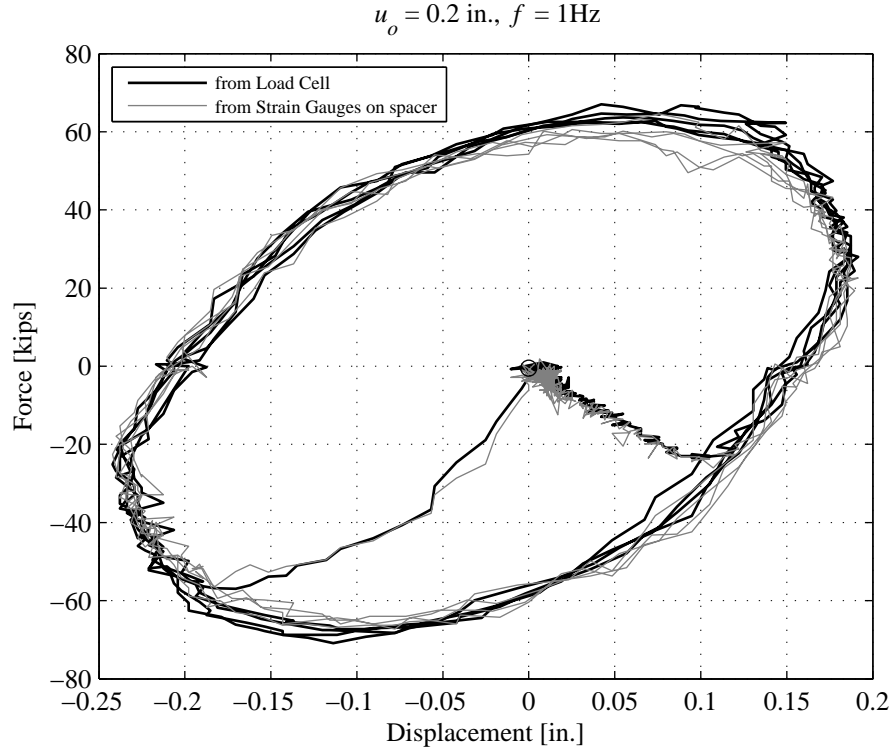


Fig. 6. Hysteresis loops with the force as measured with the load cell (heavy line) and as calculated from measured strains (light line) from strain gauges welded on the spacer.

CONCLUSIONS

This paper presented results from a comprehensive experimental program on fluid dampers in an effort to extract their force output during cyclic loading by simply measuring the strain on the damper casing and the end spacer of the damper.

The study shows that the strain gauges when installed on the damper casing can only capture the force that induces tension on the damping casing. When the piston rod is in compression the compressive force is transferred directly to the end of the damper (spacer) and only hoop stresses develop on the damper casing due to the bursting of the damper. On the other hand, the strains recorded from the spacer resulted into damper forces which are in very good agreement with the forces recorded from the load cell. The accuracy of the predictions are good even for low values of the piston stroke. The results from the experimental program indicate that with commercially available strain gauges one can monitor the force output of fluid dampers installed on the field.

ACKNOWLEDGEMENTS

This work is supported by the California Department of Transportation (CALTRANS) under grant 59A0658.

REFERENCES

- Black, C. J., and Makris, N. 2006. Viscous Heating of Fluid Dampers under Small and Large Amplitude Motions: Experimental Studies and Parametric Modeling., *Journal of Engineering Mechanics*, ASCE
- Black, C.J., and Makris, N. 2005. *Viscous Heating of Fluid Dampers Under Wind and Seismic Loading : Experimental Studies , Mathematical Modeling and Design Formulae*. Report No.EERC05. Earthquake Engineering Research Center, Berkeley, California.
- Delis, E.A., Malla, R.B., Madani, M., Thomson, K.J., et al. 1996. Energy Dissipation Devices in Bridges Using Hydraulic Dampers. *Building to Last , Proceedings, Structures Congress XIV*. Chicago, IL, 2pp.188-196.
- Makris, N. and Zhang , J. 2004. Seismic Response Analysis of Highway Overcrossings Equipped with Elastomeric Bearings and Fluid Dampers. *Journal of Structural Engineering, ASCE*, Vol.130, No. 6, pp. 830-845.
- Papanikolas, P.K. 2002. Deck Superstructure and Cable Stays of the Rion-Antirion Bridge. *Proceedings, 4th National Conference on Steel Structures*. Patras, Greece.
- Timoshenko, S.P. 1970. *Theory of Elasticity*. 3rd ed. McGraw-Hill, New York.